Clinical, histopathological and phylogenetic analysis of *Myxobolus lentisturalis* (Myxozoa: Myxobolidae) infecting the musculature of farmed population of goldfish (*Carassius auratus*) in Iran: 2021–2022

Hooman Rahmati-Holasoo[1,2*], Amin Marandi[1], Hosseinali Ebrahimzadeh Mousavi[1], Fatemeh Arabkhazaeli[3], Sara Shokrpoor[3] and Zahra Ziafati Kafi[4]

Abstract

There is a claimed increase in the global prevalence and incidence of emerging diseases observed in many organisms. Myxozoa represents an essential group of metazoan parasites that hold both economic and ecological significance. In the current study, 1% of the fish population at two commercial goldfish (*Carassius auratus*) farms in Tehran and Ghom province, Iran, developed cavitating muscular lesions resembling humps in February 2021 and January 2022. Fish displaying pathological abnormalities were transported to the Ornamental Fish Clinic and subjected to clinical examination. Light microscopy was subsequently used to examine wet smears of skin and gills, as well as whitish exudate. In addition, tissue homogenates were collected for more precise identification and molecular confirmation. The study discovered that individuals from the goldfish farms were infected with the pathogenic myxozoan *Myxobolus lentisuturalis*, which caused significant damage to the epaxial muscles. The spores collected from the humps had a lack of uniformity and were primarily ellipsoidal in shape. Histopathological analysis also revealed parasites in various stages of development, such as plasmodia and spores, as well as inflammatory cell infiltration (macrophage, giant cell and lymphoplasmacytic infiltration) between skeletal muscle fibers. Phylogenetic analysis of *M. lentisuturalis* was performed by using MEGA 11 and the maximum likelihood method. *M. lentisuturalis* is a myxozoan parasite that has been sparsely recorded and lacks widespread recognition. The current study is the first clinical, histopathological, and molecular characterization of *M. lentisuturalis* isolated from the skeletal musculature of goldfish (*C. auratus*) in Iran.

Keywords Cnidaria, Differential interference contrast, *Myxobolus lentisuturalis* myxosporea, Bivalvulida, Rhodamine

*Correspondence:
Hooman Rahmati-Holasoo
rahmatih@ut.ac.ir
[1]Department of Aquatic Animal Health, Faculty of Veterinary Medicine, University of Tehran, Tehran, Iran

[2]Centre of Excellence for Warm Water Fish Health and Disease, Shahid Chamran University of Ahvaz, Ahvaz, Iran
[3]Department of Pathobiology, Faculty of Veterinary Medicine, University of Tehran, Tehran, Iran
[4]Department of Microbiology and Immunology, Faculty of Veterinary Medicine, University of Tehran, Tehran, Iran

Introduction

Although global food production is growing rapidly through aquaculture [1, 2], modern ornamental fish farming, on the other hand, is one of the most profitable hobbies in many countries [3–8]. Goldfish (*Carassius auratus*, Linnaeus, 1758) is a freshwater cypriniform ornamental fish that has been classified into the family Cyprinidae and is native to East Asia, including China and neighboring countries [9, 10]. This fish species, originating from a natural mutation of the Crucian carp in China during the Song dynasty [11], presents a wide range of body shape and coloration [12] and is easy to domesticate as a commercial freshwater ornamental fish [11].

The global prevalence and incidence of emerging diseases are purportedly on the rise across various organisms. Gaining knowledge about the origin and causes of these diseases, as well as the organisms they affect and the possible impacts, is a crucial step in developing control and management strategies. The majority of individual fish within both wild and cultivated populations exhibit parasitic infections [13], which is posing a significant concern for the well-being of ornamental fish [14–16]. Besides the evident economic losses resulting from mortality, which may lead to the financial collapse of fish farmers, parasites can exert a substantial influence on the growth, behavior, and ultimately the reproductive fitness of ornamental fish [13, 17, 18].

The taxonomic classification Myxozoa, as proposed by Grassé in 1970, represents an essential group of metazoan parasites that hold both economic and ecological significance [19]. These parasites are predominantly benign, exhibiting complex life cycles that involve raabeia-type actinospore within the invertebrate oligochaete hosts as well as vertebrate hosts [20, 21]. The global presence of over 2,400 species belonging to 64 genera has been documented among aquatic invertebrates, fishes, amphibians, reptiles, birds, mammals, and humans [19, 22]. However, it is widely recognized that there is a significant amount of hidden diversity within this group of parasites [23]. Presently, there is a prevalent and accepted recommendation for the utilization of an integrated approach that encompasses spore morphology, precise sporulation location, host- and tissue-specificity, and molecular characteristics [24]. This approach is used for the identification of newly discovered or concealed myxosprean species, as well as for distinguishing between species that exhibit morphological similarities [25].

Among the myxozoans, the genus *Myxobolus* Bütschli, 1882, stands out as a particularly diverse genus, encompassing over 900 taxonomically described species infecting a variety of organs in a wide range of fish species throughout various geographical regions [26–29]. *Myxobolus lentisuturalis* is a myxozoan parasite that has been infrequently documented and is not widely known. This particular parasite primarily targets the skeletal muscle of fish and may cause severe pathogenic effects, leading to various health issues such as reduced growth and condition, secondary infections, respiratory distress, and mortality in the host fish [30]. *M. lentisuturalis* was described as a parasite of Prussian carp (*C. gibelio*) and goldfish (*C. auratus*) in different countries, including China [31, 32], Italy [20], the United States [33], and Hungary [34] (Table 1). This study presents the first documented occurrence of *M. lentisuturalis* in a population of commercially cultivated goldfish (*C. auratus*) in Iran. The present study provides an appropriate analysis of the morphologic and molecular characteristics of the parasite, as well as a detailed histologic description of the infection within the host.

Materials and methods

Fish source and clinical examinations

Between February 2021 and January 2022, two commercial goldfish farms in Tehran and Ghom province, Iran, developed cavitating muscular lesions that resembled humps. These lesions were distinguished by their expansile nature, occasional ulceration, and precise location on

Table 1 Comparison of morphometric characteristics and measurements of *Myxobolus Lentisuturalis* in gibel carp (*C. Gibelio*) and goldfish (*C. Auratus*) as the host fish species according to past studies and the current study

	Dyková et al. [31]	Caffara et al. [20]	Wang et al. [32]	Keeney et al. [33]	Suhaimi et al. [34]	Present study
Host species	Gibel Carp	Goldfish	Goldfish	Goldfish	Gibel Carp	Goldfish
Origin	China	Italy	China	USA	Hungary	Iran
TO	Muscle tissue	Muscle tissue	Gall bladder	Muscle Tissue	Muscle tissue	Muscle tissue
SL	11.8 (11.2–12.4)	10.5 (9.0–11.0)	11.9 (10.4–12.9)	11.4 (10.4–12.5)	11.8 (10.0-13.3)	11.2 (10.2–13.6)
SW	7.6 (7.2–8.4)	6.6 (6.0–7.0)	7.3 (6.4–7.9)	7.1 (6.4–8)	7.6 (6.6–8.6)	6.8 (6.6–7.4)
ST	5.2	3.9 (3.0–5.0)	-	4.7 (3.9–5.5)	5.0 (4.1–5.6)	4.4 (3.3–5.4)
PCL	4.2 (4.0–4.4)	3.7 (3.0–4.5)	4.1 (3.4–5.0)	4 (3.5–4.5)	4.3 (3.3–5.1)	4.1 (3.5–4.6)
PCW	2.5 (2.0–2.8)	2.2 (2.0–3.0)	2.4 (1.8–2.8)	2.6 (2.2–3)	2.7 (1.7–3.2)	2.55 (2.5–2.7)
NPFC	4	4–5	4–5	4–5	4–5	4–5

Note All measurements in this study are expressed in micrometers (µm), with the range specified within parentheses. Any data that was not available or could not be obtained is denoted by a dash (–). TO: Target organ; SL: Spore length; SW: Spore width; ST: Spore thickness; PCL: Polar capsule length; PCW: Polar capsule width; NPFC: Number of polar filament coils

the dorsal midline, just caudal to the head (Fig. 1a-d). Approximately 1% of the individuals in each pond were affected. The fish were kept in concrete pools for three months. These ponds were supplied with tap water. The fish were fed a commercially prepared diet with 31% crude protein, 5.5% crude fat, 6% crude fiber, 9% ash, and 1.5% phosphorus. This diet was given to the fish six days a week (2–3% of the body weight daily). In addition, the pond's water quality parameters, such as pH, dissolved oxygen, and temperature, were within normal limits. According to the owners' statement, the fish were purchased from the earthen ponds of goldfish farms in the north of Iran. The presence of lesions was not visible in the fry, but became apparent when the goldfish reached a size of about 7 cm. There have been no reported fatalities associated with these lesions and there had been no additional fish introduced into the system prior to the outbreak. A total of 20 goldfish (10 fish per farm) ranging in length from 7 to 15 cm were carefully placed in water-filled plastic bags. The bags were outfitted with oxygen supplies to ensure the fish's well-being during transportation. The goldfish were then transported to the Ornamental Fish Clinic, Faculty of Veterinary Medicine at the University of Tehran in Tehran, Iran.

Parasitological examinations

Clinical examination of the fish was followed by the preparation of wet smears of skin and gills, as well as whitish exudate from skeletal muscles. Wet smears were also stained with Giemsa and examined using a light microscope (Nikon, E600). The examination of myxospore-containing wet mounts was performed using differential interference contrast (DIC) microscopy, specifically a Nikon Eclipse 600 research microscope. Wet smears were also stained with rhodamine and examined under a Nikon E600 fluorescence microscope. The digital images were captured using a microscope-mounted digital camera (Tucsen, GT12) with a 100× oil immersion objective. Subsequently, spore measurements were obtained directly from these digital images using Axiovision version 4.8.

The fish were euthanized with an overdose of PI222 (Pars Imen Daru, Iran) (10 ml/10 lit), a substance with Eugenol, Carvacrol, and Eugenol acetate as major active ingredients. Following euthanasia, postmortem examinations were performed under sterile conditions. Bacterial cultures from the liver, spleen, kidney, and muscle lesions were streaked on blood agar plates and incubated at 25 °C for 96 h. A Pasteur pipette was also used to extract a whitish exudate from the swollen tissue, which contained a cluster of myxospores. The collected samples were then
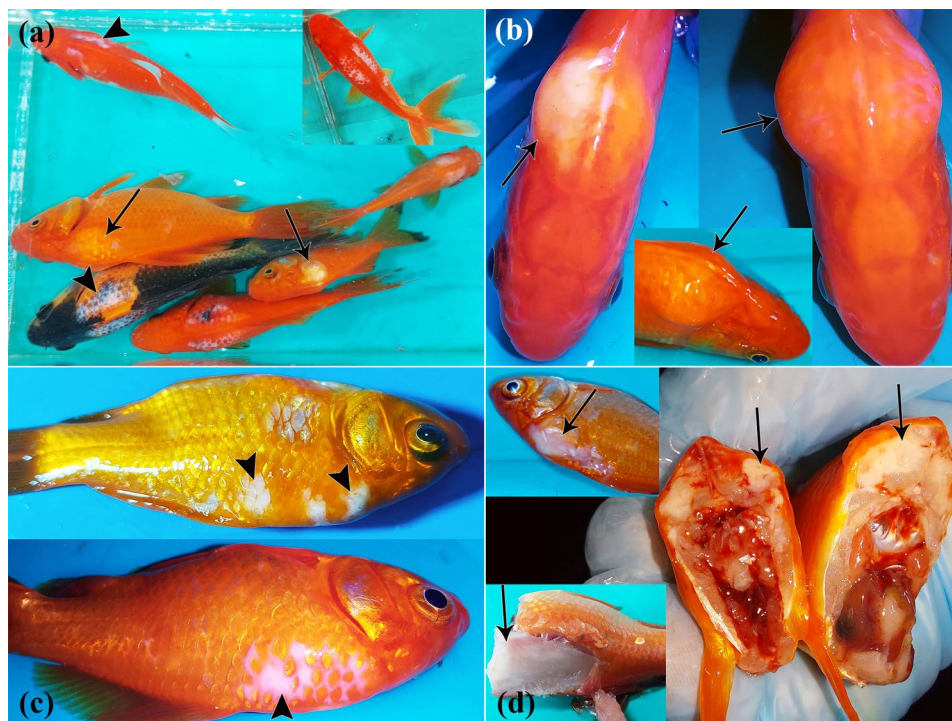

Fig. 1 Gross lesions caused by *M. lentisuturalis* infection in goldfish (*C. auratus*). (**a**-**c**) Whitish lesions on the skin (arrowheads). Note the expansile, bilobulated, hump-like, ovoid subcutaneous lesions on both sides of the dorsal midline, just caudal to the head (arrows). (**d**) Epaxial muscle whitening is evident in various cut sections (arrows)

transferred to Eppendorf tubes containing 70% ethanol for further molecular analysis.

Histopathological analysis
Various internal organs, including the kidney, intestine, gallbladder, liver, heart, brain, gill, muscle, spleen, swim bladder, and gonads, were fixed in 10% neutral buffered formalin for histological examination. These organs were then dissected, dehydrated with a series of ethanol solutions, and finally prepared for paraffin embedding using a paraffin tissue processor and dispenser. Following that, sections were sliced at a thickness of 4 µm and stained with haematoxylin-eosin (H&E). The sections of formalin-fixed muscles were also stained with Gram, Masson's trichrome (MT), Ziehl-Neelsen and periodic acid-Schiff (PAS) staining. The sections were examined using light microscopy (E600, Nikon), and representative images were captured with a microscope camera (GT12, Tucsen, Mosaic 3.0 software). To apply the image scale bars, Axiovision version 4.8 software was used, and the images were processed using Adobe Photoshop CC 2023. The section of some muscles was scanned with Mosaic 3.0 software (TrueChrome Metrics microscope camera, Tucsen).

DNA extraction and polymerase chain reaction (PCR)
DNA was extracted directly from the homogenates of affected tissues using the MBST DNA extraction kit, following the instructions provided by the manufacturer, Molecular Biological System Transfer, Iran. The extracted DNA samples were then stored at a temperature of -20 ∘C until further analysis. The amplification procedure involved the utilization of the nested PCR technique, specifically targeting the 18 small ribosomal DNA (18 S rDNA) sequence (1090 bp). The primers MC5-F (5′-C TGAGAAACGGCTACCACATCCA-3′) and MC5-R (5′-ATTAGCCTGACACATCACTCCACGA −3′) were employed in the current study. The polymerase chain reaction (PCR) was conducted by initiating a denaturation step at a temperature of 95 °C for 3 min. This was followed by a series of 35 cycles of 95 °C for 30 s, 60 °C for 30 s, and 72 °C for 30 s. The PCR process concluded with a final extension step at 72 °C for a period of 7 min.

Sequencing, bioinformatics, and phylogenetic analysis
The PCR products that yielded positive results were subjected to individual sequencing and subsequent analysis using Chromas 2.6.5 software. The software GenSAS v6.0 was utilized to carry out gene annotation and sequence trimming. A minimum threshold of 1090 base pairs (bp) of high-quality sequence, determined through the size of the fluorescence signal and the clarity of the peak, was desired. The nucleotide and amino acid sequences were subjected to analysis using CLC viewer version 8.0. The 18s rDNA sequence was obtained from GenBank, and

subsequently converted into a FASTA dataset. The edited and assembled sequences were subjected to BLASTN analysis using the National Center for Biotechnology Information (NCBI) website (https://blast.ncbi.nlm.nih.gov/). The generation of multiple sequence alignments was performed using the ClustalW algorithm. These alignments were then utilized to construct distance matrices using the Maximum Likelihood (ML) model, which was implemented in the MEGA 11 [35]. The Neighbor-Joining method trees were generated using MEGA 11, employing a 1000-fold bootstrap method.

Results
Clinical findings and laboratory examinations
No bacterial growth observed on blood agar, MacConkey agar and Trypticase Soy Agar. The bilateral crescent-shaped humps observed between the head and the dorsal fin (Fig. 1a, b) provided clear evidence of an infection caused by the extremely pathogenic myxozoan, *M. lentisuturalis*. In addition, the enlarged tissue was filled with creamy, thick, white fluid (Fig. 1c &d) containing debris from damaged muscle cells and a significant amount of myxospores (Fig. 2a). No other lesions and abnormalities were noted.

Parasitological examinations
The polar capsules of spores were stained with Giemsa (Fig. 2b). The morphology of the spores collected from the humps exhibited a lack of uniformity. The majority of the spores (more than 98%) displayed an ellipsoidal shape, characterized by symmetrical shell valves. Furthermore, it was found that the sporoplasm was mostly located in the posterior half of the body of the spore (Figs. 2a-d, 3a and 4b). The mean length of the spores was 11.2 (range: 10.2–13.6) µm, whereas the mean width was 6.8 (range: 6.6–7.4) µm. Also, the spore thickness measured 4.4 (3.3–5.4) µm (Table 1). The anterior pole of the organism featured two polar capsules that were roughly equal in size. These capsules exhibited a pyriform shape and tapered towards the anterior end (Figs. 2a-d and 4b). The mean length of the polar capsule was 4.1 (with a range of 3.5–4.6) µm, while the width measured 2.55 (with a range of 2.5–2.7) µm (Table 1). Additionally, the polar tubules exhibited a coiling pattern of 4–5 turns (Figs. 2a-d and 4b) and the mean length of the extruded polar filaments (Fig. 3a) was 100 (with a range of 98–103) µm. Rhodamine staining of wet smears enhanced the visibility of the spores and polar filaments of *M. lentisuturalis* (Fig. 3a & b). In addition to the normal spores of *M. lentisuturalis*, a few atypical spores exhibiting distinct morphological characteristics were also identified. The atypical spores were round in shape with 1–2 polar capsules (Fig. 3c), round in shape with three polar capsules (Fig. 3b), with a single forked tail (Fig. 3b), spores with
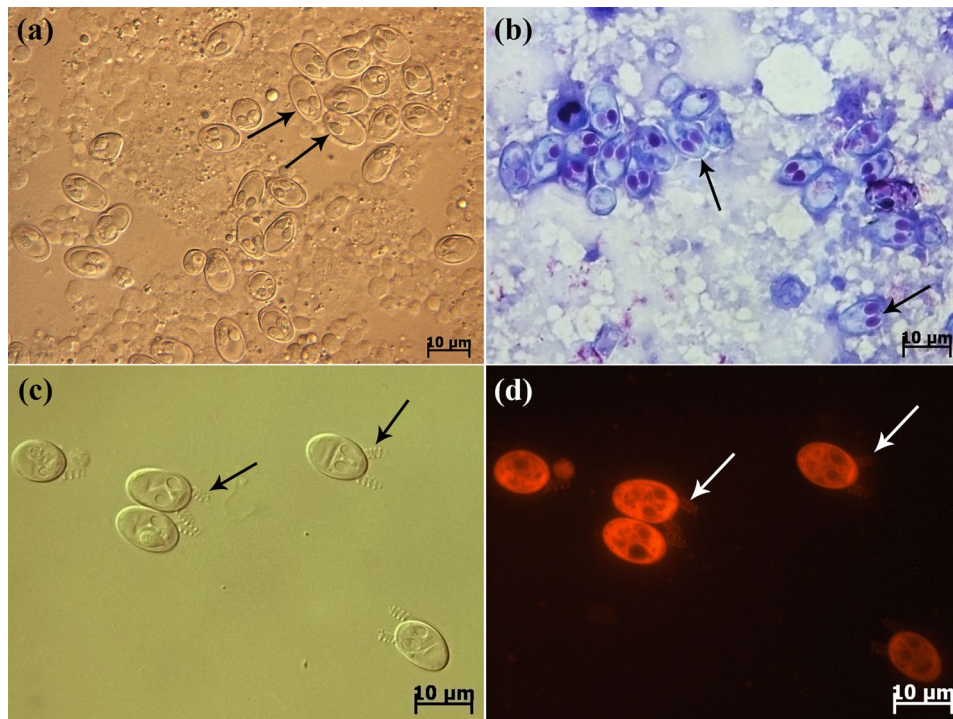
Fig. 2 (**a**) Nomarski's differential interference contrast image. Wet smear of mature *M. lentisuturalis* spores in frontal view under a light microscope (arrows). (**b**) *M. lentisuturalis* mature spores stained with Giemsa. (**c**) Extruded polar filaments of *M. lentisuturalis* (arrows). (**d**) A fluorescence microscopy image. Rhodamine-stained extruded polar filaments of *M. lentisuturalis* (arrows)
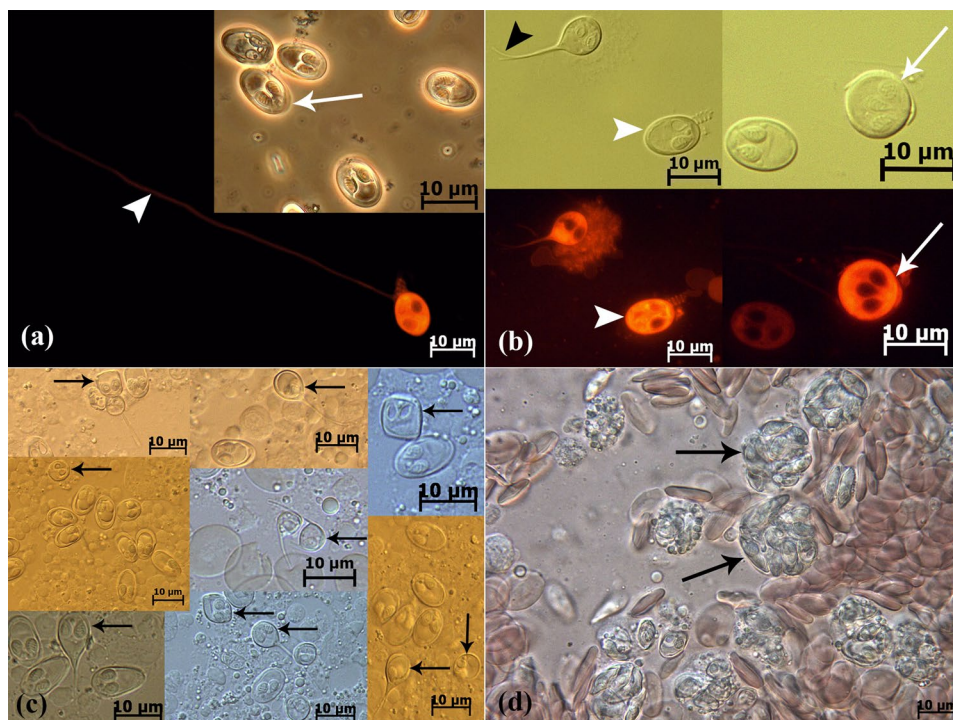

Fig. 3 (**a**) Fluorescence microscopy image of an extruded polar filament (arrowhead) from *M. lentisuturalis* stained with rhodamine. A phase contrast microscopy image of normal mature spores (arrow). (**b**) DIC and fluorescence microscopy images show spores with a single forked tail (black arrowhead) and three polar capsules (arrows). Note the normal mature spore of *M. lentisuturalis* in frontal view. Rhodamine-stained spore (white arrowhead). (**c**) Nomarski differential interference contrast images. Different spore morphotypes (arrows) are seen. (**d**) Immature spores are seen in the plasmodia (arrow)
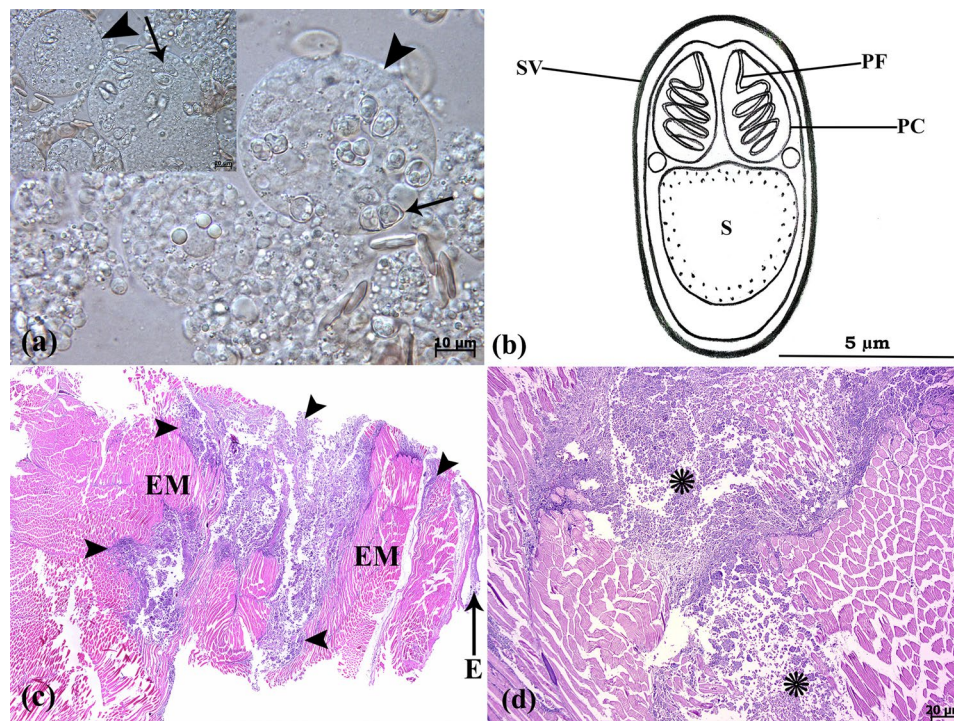
Fig. 4 Different stages of spore (arrows) formation in the plasmodia (arrowheads) are seen (Nomarski *DIC image)*. (**b**) Schematic drawing of mature spore of *M. lentisuturalis* (Frontal view). Spore valve (SV), polar filament (PF), polar capsule (PC) and S (Sporoplasm). (**c**) Scanned image of vertical cross-section of muscular hump showing large area of presence of parasites between the epaxial muscle fibers (EM). Epidermis (E) (H&E). (**d**) Diffuse granulomatous myositis (asterisks) is seen (H&E)

appendages at right angles, spores with a single appendage, and quadrangular-shaped spores (Fig. 3c). Also, some atypical spores with morphology similar to that of a *Henneguya* species were infrequently observed in the wet mounts of the cavitating muscle lesions (Fig. 3c). The dorsolateral (epaxial) muscle experienced significant damage due to the direct mechanical pressure placed on the surrounding cells or tissues caused by the enlarged pseudocysts. These pseudocysts were comprised of many plasmodia that were filled with developing spores (Figs. 3d and 4a).

Histopathological analysis

Microscopically, the tissue lesion was composed of diffuse granulomatous myositis without a distinct capsule. Histopathological examination revealed parasites at various stages of development, including plasmodia and spores, and inflammatory cell infiltration (macrophage, giant cell and lymphoplasmacytic infiltration) between the skeletal muscle fibers. The muscle layer was markedly expanded by inflammatory cells and parasites which compressed the adjacent muscle fibers and resulted in their atrophy and necrosis (Figs. 4c and d and 5a and b). This inflammation had few lymphocytes and plasma cells, numerous macrophages and multinucleated giant cells (Fig. 5c). Microscopically, most sections revealed spore-containing macrophages (Fig. 5d). Spores were refractile and difficult to see in hematoxylin and eosin sections, but polar capsules showed intense Ziehl-Neelsen staining. Spore valves were acid-fast positive, and polar capsules were mostly stained blue with Ziehl-Neelsen (Fig. 6a). The polar capsules of the spores were pink with periodic acid-Schiff (PAS) staining (Fig. 6b), moderately purple with Gram (Fig. 6c), and colorless to pale blue-gray with Masson's trichrome (MT) (Fig. 6d). Histopathological studies revealed normal tissue architecture in all internal organs (liver, kidney, spleen, intestine, gonads and heart).

Molecular and phylogenetic analysis

In this study the obtained nucleotide sequences of the 18 S rDNA of *M. lentisuturalis* were approximately 1090 bp long. They were deposited with GenBank under the accession numbers OR632226 and OR632278 and compared with the previous sequences of *M. lentisuturalis* in GenBank. Our first 18 S rDNA sequence showed high identity (≥98.5%) with the sequences from goldfish in China (AY119688) (31). Moreover, the second 18 S rDNA sequence revealed the highest similarity (≥99.9%) with the sequences from goldfish in China (AY119688 and MF150547), Italy (AY278563), the USA (OP374272), and Hungary (OR416133) (20,31–34) (Fig. 7; Table 2).
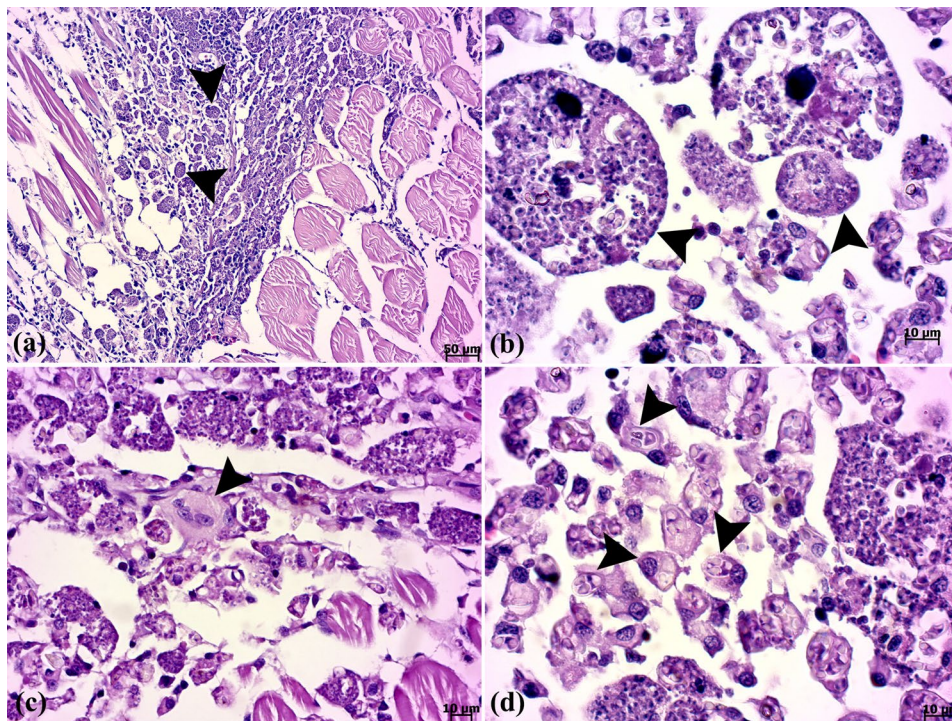
Fig. 5 Histopathological lesions associated with *M. lentisuturalis* in the musculature. (**a**-**b**) Note the myxozoan plasmodia (arrowheads). (**c**) Multinucleated giant cells (arrowhead) and (**d**) spore-containing macrophages (arrowheads) are seen (H&E)
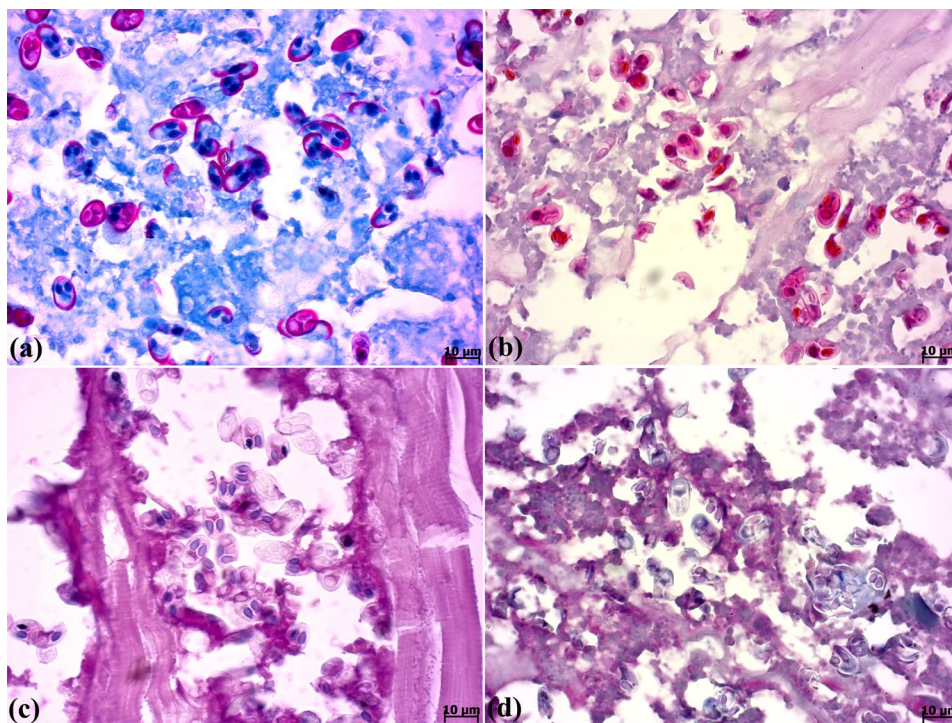

Fig. 6 Histochemical staining findings of myxozoan spore valves and polar capsules. (**a**) The shell valves of all myxozoans are strongly stained pink and the polar capsules are mostly stained deep blue (Ziehl–Neelsen stain). (**b**) The shell valves of myxozoans are strongly stained pink (periodic acid-Schiff (PAS) stain) (**c**) Polar capsules within mature myxospores are mostly stained deep purple (Gram stain). (**d**) Polar capsules within mature myxospores are stained blue-gray (Masson's trichrome stain)
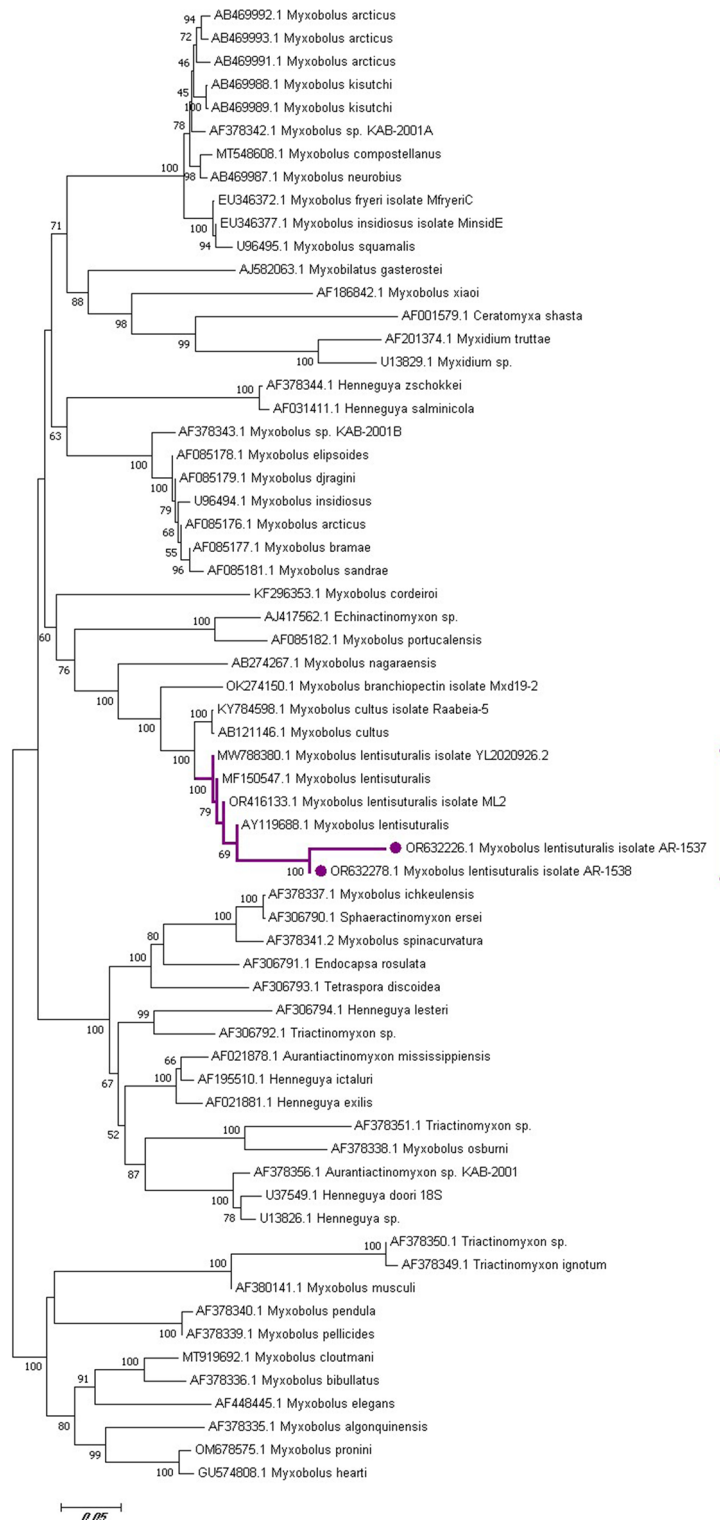
Fig. 7 Molecular phylogenetic analysis based on the nucleotide sequences of the 18 S rDNA using the Neighbor-joining method based on the Maximum likelihood model. Evolutionary analyses were performed in MEGA7. The bootstrap consensus tree derived from 1000 replicates represents the evolutionary history of the taxa analyzed. The percentage of trees in which the associated taxa were clustered together is indicated next to the branches. The tree is drawn to scale, with the length of branches measured in the number of substitutions per site

Table 2 The genetic homology between *Myxobolus Lentisuturalis* and other selected Myxobolidae was calculated using the maximum likelihood substitution model based on the 18 S rDNA

	1	2	3	4	5	6	7	8	9	10	11	12	13	14
1 OR632278.1_Myxobolus_lentisuturalis_isolate_AR-1538														
2 OR632226.1_Myxobolus_lentisuturalis_isolate_AR-1537	98.97													
3 MF150547.1_Myxobolus_lentisuturalis	100.00	90.91												
4 OR416133.1_Myxobolus_lentisuturalis_isolate_ML2	100.00	90.91	100.00											
5 AY119688.1_Myxobolus_lentisuturalis	100.00	90.92	100.00	100.00										
6 MW788380.1_Myxobolus_lentisuturalis_isolate_YL2020926.2	100.00	90.86	100.00	100.00	100.00									
7 KY784598.1_Myxobolus_cultus_isolate_Raabeia-5	96.55	87.12	97.13	97.13	97.13	97.12								
8 OK274150.1_Myxobolus_branchiopectin_isolate_Mxd19-2	88.50	78.41	90.48	90.48	90.48	90.43	90.51							
9 AB274267.1_Myxobolus_nagaraensis	80.06	68.87	83.44	83.44	83.44	83.64	83.05	81.98						
10 KF296353.1_Myxobolus_cordeiroi	71.09	60.42	72.40	72.40	72.40	72.24	72.08	73.29	69.10					
11 AB469993.1_Myxobolus_arcticus	69.28	56.70	72.08	72.08	72.08	72.09	72.28	71.68	69.53	69.20				
12 AB469987.1_Myxobolus_neurobius	68.87	56.29	71.75	71.75	71.75	71.76	71.77	71.19	69.31	68.94	97.13			
13 AF085178.1_Myxobolus_ellipsoides	68.63	56.97	72.81	72.81	72.81	73.05	71.63	71.51	71.57	71.35	76.54	76.73		
14 AJ582063.1_Myxobilatus_gasterostei	65.40	54.59	70.02	70.02	70.02	70.21	69.36	68.48	68.78	66.69	73.76	74.45	75.71	

Discussion

The present study aims to provide the first description of a highly pathogenic myxozoan parasite *M. lentisuturalis* within 2 commercial goldfish farms in Iran. A considerable number of documented species have been identified and characterized exclusively through the examination and analysis of spore morphology. The significance of myxospore morphology in identification cannot be denied, as it serves as a fundamental diagnostic characteristic. However, notable inconsistencies have been observed in the phylogenetic relationships of myxospores as inferred from the taxonomy of spore-based myxobolids [36]. According to [37], the utilization of morphological tools has proven ineffective in distinguishing congeneric species, particularly in cases where these species are present in the same infection site within different fishes and exhibit only slight differences in their morphology and spore structures. The resolution of these issues has been facilitated through the utilization of various molecular markers, with a particular emphasis on small subunit ribosomal DNA (SSU rDNA). This marker has been widely employed to identify and investigate the phylogeny of myxosporean parasites found in fish populations worldwide. Currently, there is a widely accepted approach for taxonomic assessment of myxosporean species and differentiation of species with similar morphology. This approach which involves the integration of various factors such as spore morphology, sporulation site, tissue and host specificity, and molecular characteristics, has resulted in *M. lentisuturalis* being classified into the phylum Cnidaria, class Myxosporea, order Bivalvulida, and family Myxobolidae [22, 36, 38].

M. lentisuturalis has been documented in some countries as a pathogenic myxozoan that infects the dorsal epaxial musculature of gibel carp and goldfish (Table 1). This finding is consistent with previous research that found a protrusive dorsolateral deformation in goldfish infected with this parasite in Iran. The findings obtained from the goldfish in the present study provide additional evidence that infection of muscular tissue is the predominant manifestation observed in cyprinid species infected with *M. lentisuturalis*.

DIC light microscopy confirmed that the morphological features of myxospores described herein were consistent with the previous descriptions of *M. lentisuturalis* reported by [20, 31–34]. However, comparative analysis of morphometric measurements revealed that myxospores described by [20] exhibited a slightly smaller size compared to others (Table 1). The influence of host species, tissue specificity, habitat preference, and geographical distribution on morphological and morphometric variations of parasites is widely acknowledged in the field of science [34]. The morphological characteristics observed in this study, including the dimensions of the

spore and polar capsule, the absence of a sutural ridge, and the presence of four coils in the polar filament, serve as distinguishing features that differentiate *M. lentisuturalis* from resembled species (e.g., *M. cultus*, *M. gayerae*, *M. cycloides*, *M. fundamentalis*, and *M. rutili*) [20, 31, 33]. Fluorescent staining of wet smears of fish protozoan parasites has received limited attention [39]. However, as previously recommended by [40] and [41], the current study demonstrated that using rhodamine for staining can greatly enhance the visibility of the spores and polar filaments of *M. lentisuturalis*, aiding in their study and identification.

In myxosporean infections, especially in association with species infecting the muscle the presence of dispersed spores in various organs is well known. However, meticulous microscopic examinations in the present study did not reveal any myxospores in intestinal tissues, which was in contrast with the findings of [42] who provided evidence that myxospores originating from damaged muscle cells can be transported through the bloodstream to different organs and subsequently expelled from the fish through the urinary tract, gallbladder, intestine, gills, and skin. In contrast to the findings of [34], our observations did not reveal any indications of demarcation in muscles that were substantially impacted, which was in concurrence with the findings of [31]. Furthermore, the identification of *M. lentisuturalis* myxosporean developmental stages was mainly limited to the epaxial skeletal muscle, aligning with the observations made by [34]. In a study conducted by [33], it was discovered that spores were also present in the epidermis.

The detection of myxosporidian infection through the application of polymerase chain reaction (PCR) is widely regarded as a highly reliable diagnostic method for identifying the presence of the parasite. It is essential to include molecular analysis of sequence data (e.g., ribosomal genes) in all descriptions of myxozoans, not only for evaluating the phylogenetic relationships among species but also for assessing the reliability of spore morphology [34]. This study revealed that the sequence of Tehran samples was completely identical to the China [31] samples (a similarity of ≥98.5%), and the sequence of Ghom samples was completely identical to the China [32], Italy [20], the USA [33], and Hungary [34] samples (a similarity of ≥99.9%).

According to prior studies, it has been established that the goldfish host becomes infected via an intermediate oligochaete host, specifically *Branchiura sowerbyi*, rather than through direct transmission [20, 31]. This outbreak is most likely attributed to the presence of earthen ponds and the potential favorable conditions for oligochaete development on the farm, making these aquatic worms the primary source of infection. While there have been no recorded instances of fatalities caused by *M. lentisuturalis*, the persistence of infection over an extended period or its recurrence within a farmed population could result in substantial financial losses due to the parasite's ability to cause deformities. Furthermore, it should be noted that asymptomatic goldfish, which are commonly traded in the ornamental fish industry, possess the capacity to transmit the parasite to various environments and other fish species, thereby contributing to the dissemination of the parasite [33]. The use of a strategy aimed at interrupting the evolutionary life cycle of myxozoan parasites through the elimination of the intermediate host can be regarded as a potentially effective approach to management [43]. In addition, the implementation of culling measures targeting individuals displaying visible signs of infection has proven to be a successful approach for managing this parasite. However, it is imperative to conduct ongoing surveillance of outbreaks and carefully document any potential reappearances in order to effectively reduce the severity of future outbreaks and minimize the economic impact caused by this parasite [33].

Conclusion

To the best of our knowledge, this study represents the first clinical, histopathological, and molecular characterization of *M. lentisuturalis* from goldfish (*C. auratus*) in Iran. Based on the findings of the present study, additional research is warranted to elucidate the specific mechanisms underlying the pathogenesis of *M. lentisuturalis* in cyprinid fish. Also, the need for increased consideration of diverse strategies aimed at preventing the dissemination of myxospora infections to novel geographic regions and their introduction into previously uninfected fish species is evident.

Data availability
No datasets were generated or analysed during the current study.

Declarations

Ethics approval and consent to participate
In the current study, clinical records were provided following the consent of owners and all protocols were approved by Research Ethics Committees of Faculty of Veterinary Medicine- University of Tehran (Approval ID: IR.UT.

VETMED.REC.1402.003). All methods were carried out in accordance with relevant guidelines and regulations of the University of Tehran Veterinary Ethical Review Committee. Written informed consent was obtained from the owners for the participation of the animals in the study.

Consent for publication
Not applicable.

Competing interests
The authors declare no competing interests.

References

1. Ahmadivand S, Weidmann M, El-Matbouli M, Rahmati-Holasoo H. Low pathogenic strain of infectious pancreatic necrosis virus (IPNV) associated with recent outbreaks in Iranian trout farms. Pathogens. 2020;24:782. https://doi.org/10.3390/pathogens9100782.
2. Anderson JL, Asche F, Garlock T, Chu J, Aquaculture. Its role in the future of food. In: Schmitz A, Kennedy PL, Schmitz TG, editors. World Agricultural resources and Food Security: International Food Security. Emerald Publishing Limited; 2017. pp. 159–73. https://doi.org/10.1108/S1574-871520170000017011.
3. Livengood EJ, Chapman FA. The ornamental Fish Trade: an introduction with perspectives for responsible Aquarium Fish Ownership: FA124/FA124, 5/2007. Edis. 2007;16:1–8.
4. Rahmati-Holasoo H, Ahmadivand S, Marandi A, Shokrpoor S, Palić D, Jahangard A. Identification and characterization of lymphocystis disease virus (LCDV) from Indian glassy fish (*Parambassis ranga* Hamilton, 1822) in Iran. Aquacult Int. 2022;30:2593–602. https://doi.org/10.1007/s10499-022-00922-7.
5. Rahmati-Holasoo H, Marandi A, Mousavi HE, Azizi A. Isolation and identification of *Capillaria* sp. in ornamental green terror (*Andinoacara Rivulatus* Günther, 1860) farmed in Iran. Bull Eur Association Fish Pathologists. 2022;43:12–20. https://doi.org/10.48045/001c.39773.
6. Rahmati-Holasoo H, Ghalyanchilangeroudi A, Kafi ZZ, Marandi A, Shokrpoor S, Imantalab B, Mousavi HE. Detection of lymphocystis disease virus (LCDV) from yellowbar angelfish (*Pomacanthus maculosus* Forsskål, 1775) in Iran: histopathological and phylogenetic analysis. Aquaculture. 2023;562:738862. https://doi.org/10.1016/j.aquaculture.2022.738862.
7. Rahmati-Holasoo H, Niyyati M, Fatemi M, Mahdavi Abhari F, Shokrpoor S, Nassiri A, Marandi A. Molecular identification, phylogenetic analysis and histopathological study of pathogenic free-living amoebae isolated from discus fish (*Symphysodon Aequifasciatus*) in Iran: 2020–2022. BMC Vet Res. 2024;20:54. https://doi.org/10.1186/s12917-024-03902-6.
8. Shokrpoor S, Rahmati Holasoo H, Soroori S, Marandi A, Imantalab B. Basal cell carcinoma in an albino pindani (*Chindongo Socolofi*) and a cobalt-zebra (*Maylandia Callainos*): diagnostic imaging, clinical and histopathological study. J Fish Dis. 2022;45:1251–8. https://doi.org/10.1111/jfd.13657.
9. Nelson JS. Fishes of the world. Hoboken, NJ: Wiley; 2006.
10. Sood N, Swaminathan TR, Yadav MK, Pradhan PK, Kumar R, Sood NK. First report of cutaneous infiltrative lipoma in goldfish *Carassius auratus*. Dis Aquat Organ. 2017;125:243–7. https://doi.org/10.3354/dao03148.
11. Komiyama T, Kobayashi H, Tateno Y, Inoko H, Gojobori T, Ikeo K. An evolutionary origin and selection process of goldfish. Gene. 2009;430:5–11. https://doi.org/10.1016/j.gene.2008.10.019.
12. Brewster B, Fletcher N. Keeping Goldfish. Interpret publishing; 2004.
13. Rahmati-Holasoo H, Marandi A, Ebrahimzadeh Mousavi H, Taheri Mirghaed A. Parasitic fauna of farmed freshwater ornamental fish in the northwest of Iran. Aquacult Int. 2022;30:633–52. https://doi.org/10.1007/s10499-021-00832-0.
14. Jerônimo GT, Marchiori ND, Pádua SB, Dias Neto J, Pilarski F, Ishikawa MM, Martins ML. *Trichodina colisae* (Ciliophora: Trichodinidae): new parasite records for two freshwater fish species farmed in Brazil. Revista Brasileira De Parasitol Veterinária. 2012;21:366–71. https://doi.org/10.1590/S1984-29612012005000008.
15. Rahmati-Holasoo H, Marandi A, Shokrpoor S, Goodarzi T, Ziafati Kafi Z, Ashrafi Tamai I, Ebrahimzadeh Mousavi H. Clinico-histopathological and phylogenetic analysis of protozoan epibiont *Epistylis wuhanensis* associated with crustacean parasite *Lernaea cyprinacea* from ornamental fish in Iran. Sci Rep. 2023;13:14065. https://doi.org/10.1038/s41598-023-41368-y.
16. Rahmati-Holasoo H, Tavakkoli S, Ebrahimzadeh Mousavi H, Marandi A, Taheri Mirghaed A. Parasitic fauna of farmed freshwater ornamental sutchi catfish (*Pangasiandon hypophthalmus*) and silver dollar (*Metynnis hypsauchen*) in Alborz Province, Iran. Veterinary Med Sci. 2023;9:1627–35. https://doi.org/10.1002/vms3.1150.
17. Barber I. Parasites, behaviour and welfare in fish. Appl Anim Behav Sci. 2007;1:251–64. https://doi.org/10.1016/j.applanim.2006.09.005.
18. Barber I, Hoare D, Krause J. Effects of parasites on fish behaviour: a review and evolutionary perspective. Rev Fish Biol Fish. 2000;10:131–65. https://doi.org/10.1023/A:1016658224470.
19. Fiala I, Bartošová-Sojková P, Whipps CM. Classification and phylogenetics of Myxozoa. In: Okamura B, Gruhl A, Bartholomew JL, editors. An introduction to myxozoan evolution, ecology and development. Springer International Publishing; 2015. pp. 85–110. https://doi.org/10.1007/978-3-319-14753-6_5.
20. Caffara M, Raimondi E, Florio D, Marcer F, Quaglio F, Fioravanti ML. The life cycle of *Myxobolus Lentisuturalis* (Myxozoa: Myxobolidae), from goldfish (*Carassius auratus Auratus*), involves a Raabeia-type actinospore. Folia Parasitol (Prague). 2009;1:6. https://doi.org/10.14411/fp.2009.002.
21. Atkinson SD, Bartholomew JL, Lotan T. Myxozoans: ancient metazoan parasites find a home in phylum Cnidaria. Zoology. 2018;1. https://doi.org/10.1016/j.zool.2018.06.005. :66–8.
22. Gupta A, Chaudhary A, Tyagi A, Sharma B, Singh HS. Molecular tools for identification and classification of Myxozoan parasites (Cnidaria: Myxosporea) in India: current status. J Appl Nat Sci. 2021;13:51–8. https://doi.org/10.31018/jans.v13i1.2451.
23. Shin SP, Shirakashi S, Hamano S, Kato K, Lasso LT, Yokoyama H. Phylogenetic study of the genus *Kudoa* (Myxozoa: Multivalvulida) with a description of *Kudoa rayformis* sp. nov. from the trunk muscle of Pacific Sierra *Scomberomorus sierra*. Mol Phylogenet Evol. 2016;98:337–45. https://doi.org/10.1016/j.ympev.2016.02.019.
24. Liu XH, Batueva MD, Zhao YL, Zhang JY, Zhang QQ, Li TT, Li AH. Morphological and molecular characterisation of *Myxobolus pronini* n. sp. (Myxozoa: Myxobolidae) from the abdominal cavity and visceral serous membranes of the gibel carp *Carassius auratus Gibelio* (Bloch) in Russia and China. Parasites Vectors. 2016;9:1–1. https://doi.org/10.1186/s13071-016-1836-3.
25. Atkinson SD, Bartošová-Sojková P, Whipps CM, Bartholomew JL. Approaches for characterising myxozoan species. Myxozoan Evol Ecol Dev. 2015;111:23. https://doi.org/10.1007/978-3-319-14753-6_6.
26. Velasco M, Matos P, Sanches O, São Clemente SC, Videira M, Santos P, Matos E. Necrotizing myositis associated with parasitism by *Myxobolus* sp. (Myxozoa) in the palate of the violet goby, *Gobioides broussonnetii* (Gobiidae), from Marajó Island, Brazil. Aquaculture. 2012;358:129–31. https://doi.org/10.1016/j.aquaculture.2012.06.033.
27. Eiras JC, Cruz CF, Saraiva A, Adriano EA. Synopsis of the species of *Myxobolus* (Cnidaria, Myxozoa, Myxosporea) described between 2014 and 2020. Folia Parasitol. 2021;68:012. https://doi.org/10.14411/fp.2021.012.
28. Fariya N, Kaur H, Singh M, Abidi R, El-Matbouli M, Kumar G. Morphological and molecular characterization of a new myxozoan, *Myxobolus grassi* sp. nov. (Myxosporea), infecting the Grass Carp, *Ctenopharyngodon idella* in the Gomti river, India. Pathogens. 2022;28:303. https://doi.org/10.3390/pathogens11030303.
29. Mathews PD, Mertins O, Flores-Gonzales AP, Espinoza LL, Aguiar JC, Milanin T. Host–Parasite Interaction and phylogenetic of a New Cnidarian Myxosporean (Endocnidozoa: Myxobolidae) infecting a Valuative Commercialized Ornamental Fish from Pantanal Wetland Biome, Brazil. Pathogens. 2022;11:1119. https://doi.org/10.3390/pathogens11101119.
30. Lom J, Dyková I. Protozoan parasites of fishes. Elsevier Science; 1992.
31. Dyková I, Fiala I, Nie P. *Myxobolus lentisuturalis* sp. n. (Myxozoa: Myxobolidae), a new muscle-infecting species from the prussian carp, *Carassius gibelio* from China. Folia Parasitol. 2002;49:253–8. https://doi.org/10.14411/fp.2002.048.
32. Wang M, Zhao Y, Yang C. The impacts of geographic and host species isolation on population divergence of *Myxobolus Lentisuturalis*. Parasitol Res. 2019;118:1061–6. https://doi.org/10.1007/s00436-019-06234-9.
33. Keeney CMH, Waltzek TB, de Oliveira Viadanna PH, Frasca S Jr, Reinhardt E, Lovy J, et al. *Myxobolus lentisuturalis* infection in a farmed population of goldfish *Carassius auratus* from the USA. Dis Aquat Organ. 2023;154:7–14. https://doi.org/10.3354/dao03735.
34. Suhaimi NS, Colunga-Ramírez G, Sellyei B, Cech G, Molnár K, Székely C. The first detection of *Myxobolus Lentisuturalis* Dyková, Fiala Et Nie, 2002, a highly pathogenic muscle-infecting parasite of gibel carp (*Carassius auratus* Gibelio Berg, 1932) in Hungary. J Fish Dis. 2023;46:1367–76. https://doi.org/10.1111/jfd.13855.

35. Tamura K, Stecher G, Kumar S. MEGA11: molecular evolutionary genetics analysis version 11. Mol Biol Evol. 2021;38:3022–7. https://doi.org/10.1093/molbev/msab120.

36. Fiala I, Bartošová P. History of myxozoan character evolution on the basis of rDNA and EF-2 data. BMC Evol Biol. 2010;10:1–3. https://doi.org/10.1186/1471-2148-10-228.

37. Ye L, Lu M, Quan K, Li W, Zou H, Wu S, Wang J, Wang G. Intestinal disease of scattered mirror carp *Cyprinus carpio* caused by *Thelohanellus Kitauei* and notes on the morphology and phylogeny of the myxosporean from Sichuan Province, Southwest China. Chin J Oceanol Limnol. 2017;35:587–96. https://doi.org/10.1007/s00343-017-5312-5.

38. Holzer AS, Sommerville C, Wootten R. Molecular relationships and phylogeny in a community of myxosporeans and actinosporeans based on their 18S rDNA sequences. Int J Parasitol. 2004;34:1099–111. https://doi.org/10.1016/j.ijpara.2004.06.002.

39. Alavinia SJ, Mirzargar SS, Rahmati-Holasoo H, Mousavi HE. The in vitro and in vivo effect of tannic acid on *Ichthyophthirius multifiliis* in zebrafish (*Danio rerio*) to treat ichthyophthiriasis. J Fish Dis. 2018;41:1793–802. https://doi.org/10.1111/jfd.12886.

40. Kent ML, Andree KB, Bartholomew JL, El-Matbouli MA, Desser SS, Devlin RH, Feist SW, Hedrick RP, Hoffmann RW, Khattra J, Hallett SL. Recent advances in our knowledge of the Myxozoa. J Eukaryot Microbiol. 2001;48:395–413. https://doi.org/10.1111/j.1550-7408.2001.tb00173.x.

41. Lom J, Arthur JR. A guideline for the preparation of species descriptions in Myxosporea. J Fish Dis. 1989;12:151–6. https://doi.org/10.1111/j.1365-2761.1989.tb00287.x.

42. Molnár K, Kovács-Gayer É. Experimental induction of *Sphaerospora renicola* (Myxosporea) infection in common carp (*Cyprinus carpio*) by transmission of SB-protozoans. J Appl Ichthyol. 1986;2:86–94. https://doi.org/10.1111/j.1439-0426.1986.tb00433.x.

43. Stoskopf MK. Biology and management of laboratory fishes. Fox JG. Laboratory Animal Medicine. Academic; 2015. pp. 1063–86. https://doi.org/10.1016/B978-0-12-409527-4.00021-3.

Publisher's Note